Struct Chem (2011) 22:45–56
DOI 10.1007/s11224-010-9694-7

ORIGINAL RESEARCH

Synthesis, molecular conformation, vibrational, electronic transition, and chemical shift assignments of 4-(thiophene-3-ylmethoxy)phthalonitrile: a combined experimental and theoretical analysis

Ali Coruh · Faruk Yilmaz · Busra Sengez · Mustafa Kurt · Mehmet Cinar · Mehmet Karabacak

Received: 3 July 2010 / Accepted: 10 November 2010 / Published online: 24 November 2010
© Springer Science+Business Media, LLC 2010

Abstract This work presents the synthesis and characterization of a novel compound, 4-(thiophene-3-ylmethoxy)phthalonitrile (TMP). The spectroscopic properties of the compound were examined by FT-IR, FT-Raman, NMR, and UV techniques. FT-IR and FT-Raman spectra in solid state were observed in the region 4000–400 cm^{-1} and 3500–50 cm^{-1}, respectively. The ^{1}H and ^{13}C NMR spectra were recorded in $CDCl_3$ solution. The UV absorption spectrum of the compound that dissolved in THF was recorded in the range of 200–800 nm. The structural and spectroscopic data of the molecule in the ground state were calculated using density functional theory (DFT) employing B3LYP exchange correlation and the 6-311++G(d,p) basis set. The vibrational wavenumbers were calculated and scaled values were compared with experimental FT-IR and FT-Raman spectra. The complete assignments were performed on the basis of the experimental results and total energy distribution (TED) of the vibrational modes, calculated with scaled quantum mechanics (SQM) method. Isotropic chemical shifts (^{13}C NMR and ^{1}H NMR) were calculated using the gauge-invariant atomic orbital (GIAO) method. A study on the electronic properties, such as HOMO and LUMO energies, were performed by time-dependent DFT (TD-DFT) approach. The HOMO and LUMO analyses have been used to elucidate information regarding charge transfer within the molecule. Comparison of the calculated frequencies, NMR chemical shifts, absorption wavelengths with the experimental values revealed that DFT method produces good results.

Keywords 4-(Thiophene-3-ylmethoxy)phthalonitrile · FT-IR, FT-Raman, ^{13}C and ^{1}H NMR, UV spectra · HOMO and LUMO · DFT

A. Coruh
Department of Physics, Sakarya University, 54100 Sakarya, Turkey

F. Yilmaz · B. Sengez
Department of Chemistry, Gebze Institute of Technology, 41400 Kocaeli, Turkey

M. Cinar · M. Karabacak (✉)
Department of Physics, Afyon Kocatepe University, 03040, Afyonkarahisar, Turkey
e-mail: karabacak@aku.edu.tr

M. Kurt
Department of Physics, Ahi Evran University, 40100 Kırşehir, Turkey

Introduction

Thiophene is one of the important biomolecules [1–3]. It is a heterocyclic aromatic compound and consists of a flat five-membered ring. As thiophene has a rich synthetic flexibility, it can be substituted at the 3- and 4-position. The thiophene ring, with substitution at the 3-position, can be employed in polymerization [4, 5]. Linking of thiophene rings through 2, 5 positions forms polythiophenes (PThs) and they become conductive material upon oxidation.

The structure of thiophene was thoroughly studied theoretically, as well as, experimentally in the gas phase, liquid, and solid state [6–9]. It was studied even as early as 1965 by Rico et al. [10] and the assignments of the fundamental modes were proposed. Later Klots et al. [8] made a detailed vibrational analysis of furan, pyrrole, and thiophene in vapor phase and obtained a complete set of vibrational wavenumbers of the fundamental modes of thiophene. Vibrational study of thiophene and its solvation

in two polar solvents, DMSO and methanol by Raman spectroscopy combined with ab initio and DFT calculations were studied by Singh et al. [9].

Phthalocyanines (PCs) have attracted great research attention because of their fascinating electronic and optical properties for many applications such as chemical sensors, liquid crystals, catalysis, and non-linear optics [11, 12]. These properties also strongly depend on the peripheral and axial substitution pattern. A particularly attractive feature of PCs is the possibility of tuning these properties through slight changes on the nature of the peripheral substituents or using different central metal ions in the phthalocyanine core [12, 13]. In order to overcome the insolubility of unsubstituted phthalocyanine parent molecule, peripheral groups have been extensively used to enhance solubility and, at the same time, processibility and mesophase formation. In this sense, long alkyl, alkyloxy, alkylsulfanyl or bulky apolar groups lead to soluble products in common organic solvents while anionic or cationic substituents (e.g., sulfo groups, carboxylic acids, ammonium groups) result with products soluble in aqueous media [14–16].

Phthalonitriles (PNs) are known precursors to phthalocyanines, an important class of molecules with wide applications [17], ranging from catalysis to solid-state materials. The PNs are traditionally used as dyes and pigments [18]. The polymers of PNs are also an important class of high performance polymers, which are easily processable, and display good mechanical properties, outstanding thermal and thermal-oxidative stability. Phthalonitrile polymers were firstly reported by Price and Keller [19] for aerospace, marine, and electronic packaging applications. By thermal treatment of phthalonitrile derivatives at elevated temperatures (generally high up to 350 °C) for an extended period of time, a curing reaction occurs between the nitrile groups and giving rise to a phthalonitrile polymer. The curing reaction was found to be readily promoted in the presence of a small amount of curing additives such as organic amines [19], strong organic acids [20], strong organic acids/amine salts [21], phenols [22], transition metals and their salts [23, 24], and the temperatures of the curing reaction could be greatly lowered.

Present study reports the synthesis, experimental FT-IR, FT-Raman, NMR and UV spectra, and quantum chemical calculations of 4-(thiophene-3-ylmethoxy)phthalonitrile (TMP). All spectroscopic properties which examined by the experimental techniques were supported by the computed results. In the ground state theoretical geometric parameters, IR, Raman, NMR and UV spectra, HOMO and LUMO energies of title molecule were calculated by using Gaussian 03 suite of quantum chemical codes [25], for the first time. The HOMO and LUMO analyses have been used to elucidate information regarding charge transfer within the molecule.

Materials and methods

Materials

Dimethylsulfoxide (DMSO) was freshly distilled and dried by standard methods before use. 4-nitrophthalonitrile (99.0%), 3-thiophenemethanol (98.0%), and K_2CO_3 (99.99%) were purchased from Sigma-Aldrich chemical Company (USA) and used as received.

Synthesis of 4-(thiophene-3-ylmethoxy)phthalonitrile (TMP)

4-(Thiophene-3-ylmethoxy)-phthalonitrile (**3**) was synthesized as follows [26]; a mixture of 3-thiophenemethanol (**1**) (0.57 g, 5.00 mmol), 4-nitrophthalonitrile (**2**) (0.80 g, 4.60 mmol), and dry K_2CO_3 (1.60 g, 11.60 mmol) in 40 mL dry DMSO was stirred in a two necked round bottom flask under argon atmosphere at room temperature (RT) for 2 days. Another portion of dry K_2CO_3 (1.20 g, 8.60 mmol) was added after 2 days and the reaction mixture was kept under argon atmosphere for another 5 days at RT with continuous stirring. Then, the product was precipitated out of solution by neutralizing with 0.10 M HCl to obtain a greenish precipitate. The precipitated product was finally washed twice with distilled water and recrystallized from ethanol. The resulting green solid was dried over P_2O_5 in a desiccator. Yield: 68%. mp: 85 °C.

IR (KBr disk) *wavenumbers* (cm^{-1}): 3110, 3080, 2940, 2875, 2222 (cyano), 1594 (ether), 1503, 1319 (ether), 1253, 1169, 1086, 988, 802. ^1H NMR (δ, ppm from TMS in $CDCl_3$): 5.12 (s), 7.05 (m), 7.22 (d), 7.42 (m), 7.53 (d), 7.79 (d). Electron spray mass spectra: calcd. for $C_{13}H_8N_2OS$: 240.28 *m/z*; found: 240.08 *m/z*. Anal. calcd. %: C: 64.98, N: 11.66, H: 3.36; found %: C: 64.75, N: 11.95, H: 3.30. UV–vis (THF): λ_{max}/nm (log ε): 313 (2.76) (Scheme 1).

Experimental details

The FT-IR spectrum of studied compound was recorded in the range of 400–4000 cm^{-1} on Perkin-Elmer Paragon 1000 spectrometer. Sample was prepared with thoroughly mixed KBr and pressed into disc form. FT-Raman spectrum of the sample was recorded using 1064 nm line of Nd:YAG laser as excitation wave length in the region 50–3500 cm^{-1} on a Bruker RFS 100/S FT-Raman. The detector is a liquid nitrogen cooled Ge detector. Five hundred scans were accumulated at 4 cm^{-1} resolution using a laser power of 100 mW. ^1H and ^{13}C NMR spectra were recorded in chloroform ($CDCl_3$) solution on a Varian UNITY INOVA 500 MHz spectrometer using TMS as an internal reference at 25 °C. Mass spectrum was recorded

Scheme 1 Synthesis of TMP

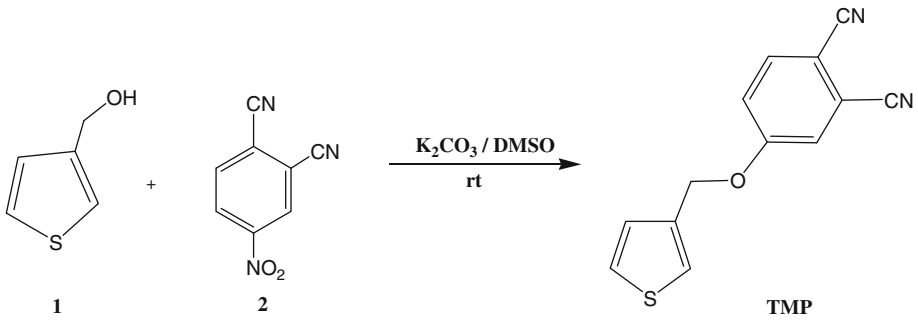

on a Bruker MicroTOF LC–MS spectrometer using the electrospray ionization (ESI) method. UV–VIS spectrum of title compound was recorded at room temperature using a Shimadzu, 2101 PC.

Quantum chemical calculations

The first task for the computational work was to determine the optimized geometry of the compound. It is well known in the quantum chemical literature that the hybrid B3LYP [27, 28] method based on Becke's three parameter functional of density functional theory (DFT) yields a good description of harmonic vibrational wavenumbers for small and medium sized molecules. Based on our previous experience [29–31] this method and a fairly large and flexible basis set 6-311++G(d,p) level to perform accurate calculations on the title molecule were chosen. Optimized structural parameters were used in vibrational wavenumbers, isotropic chemical shifts, and electronic transitions calculations. The stability of the optimized geometries was confirmed by frequency calculations, which give positive values for all the obtained frequencies. The complete vibrational assignments were performed on the basis of the total energy distribution (TED) of the vibrational modes, calculated with scaled quantum mechanics (SQM) method [32, 33]. For NMR calculations, after optimization, ^{1}H and ^{13}C NMR chemical shifts (δH and δC) were calculated using the gauge-invariant atomic orbital (GIAO) method [34, 35] in chloroform-*d* ($CDCl_3$). The GIAO method is one of the most common approaches for calculating nuclear magnetic shielding tensors. The GIAO approach allows the computation of the absolute chemical shielding due to the electronic environment of the individual nuclei and this method is often more accurate than those calculated with other approaches for the same basis set size. The electronic properties, such as HOMO–LUMO energies, dipole moment, absorption wavelengths, and oscillator strengths were calculated using B3LYP method of the time-dependent DFT (TD-DFT) [25, 36–39], based on the optimized structure. The entire calculations were performed by using Gaussian 03 [25] program package, invoking gradient geometry optimization.

Results and discussion

Molecular geometry

The title molecule consists of two rings (namely benzene and thiophene ring). The optimized structure of TMP is shown in Fig. 1 with numbering of the atoms. The optimized bond lengths, bond angles, and selected dihedral angles of compound calculated with B3LYP method and 6-311++G(d,p) basis set are listed in Table 1 in accordance with the atom numbering scheme given in Fig. 1. Since the X-ray analysis of the compound could not be done, the optimized structure can only be compared with other similar systems for which crystal structures have been solved (those of 4-(benzyloxy)phthalonitrile) [40]. From the structural data shown in Table 1 it is seen that the various bond lengths are found to be greater than experiment. This overestimation can be explained that the theoretical calculations belong to isolated molecule in gaseous phase and the experimental results belong to similar molecule in solid state. A quick look at Table 1 shows that the calculated C≡N triple-bond distances are larger than experimental results. The phthalonitrile group is coplanar with the four-atom bridge (C1–O14–C23–C15) to the thiophene group.

Vibrational spectra

The experimental and theoretical Infrared and Raman spectra of 4-(thiophene-3-ylmethoxy)phthalonitrile are shown in Fig. 2, where the calculated intensity is plotted against the wavenumbers. The observed and calculated wavenumbers along with their relative intensities, scattering activities, and probable assignments with TED of title molecule are given in Table 2. It should be noted that the calculations were made for a free molecule in vacuum,

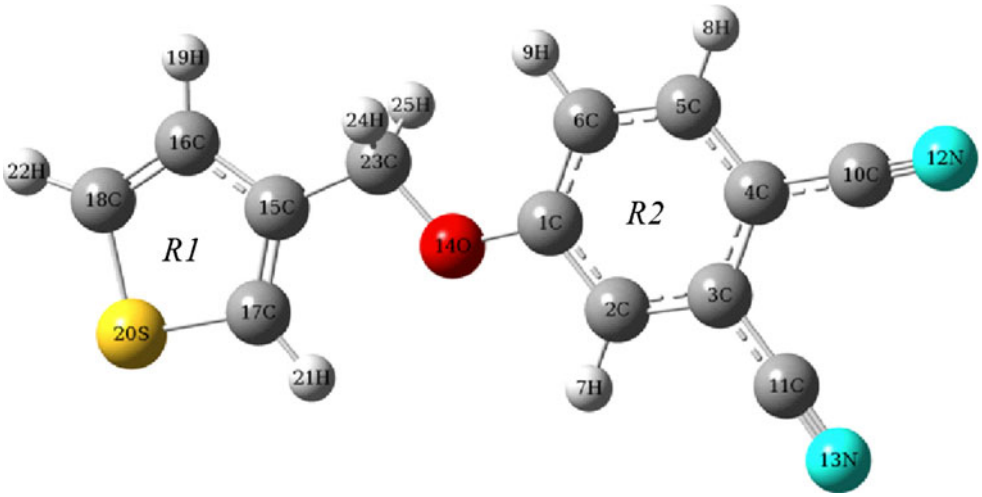

Fig. 1 The theoretical optimized geometric structure and atoms numbering of 4-(thiophene-3-ylmethoxy)phthalonitrile

while the experiments were performed for the solid samples. Furthermore, the anharmonicity is neglected in the real system for the calculated vibrations. Therefore, there are disagreements between the calculated and observed vibrational wavenumbers, and because of the low IR and Raman intensities of some modes, it is difficult to observe them in the IR and Raman spectra. The studied compound consists of 25 atoms, and so they have 69 normal vibrational modes. The numerical harmonic vibrational analysis was done for the optimized geometry, the absence of negative frequencies for the stationary points found at the molecular potential energy hypersurfaces confirming that this structure correspond to real minimum. Vibrational spectral assignments have been performed on the recorded FT-IR and FT-Raman spectra based on theoretically predicted wavenumbers and their TED.

The calculated harmonic force constants (not given in paper) and wavenumbers are usually higher than the corresponding experimental quantities because of the combination of electron correlation effects and basis set deficiencies. Nevertheless, after applying a uniform scaling factor, the theoretical calculation reproduces the experimental data well. The observed slight disagreement between theory and experiment could be a consequence of the anharmonicity and the general tendency of the quantum chemical methods to overestimate the force constants at the exact equilibrium geometry. Therefore, it is customary to scale down the calculated harmonic wavenumbers in order to improve the agreement with the experiment. In our study, we have followed two different scaling factors, i.e., 0.983 up to 1700 cm^{-1} and 0.958 for greater than 1700 cm^{-1} [41].

The Raman activities (S_{Ra}) calculated with the Gaussian 03 program [25] were converted to relative Raman intensities (I_{Ra}) using the following relationship derived from the intensity theory of Raman scattering: [42, 43].

$$I_i = \frac{f(\upsilon_0 - \upsilon_i)^4 S_i}{\upsilon_i[1 - \exp(-hc\upsilon_i/kT)]}$$

where v_0 is the laser exciting wavenumber in cm^{-1} (in this work, we have used the excitation wavenumber $v_0 = 9398.5$ cm^{-1}, which corresponds to the wavelength of 1064 nm of a Nd:YAG laser), v_i the vibrational wavenumber of the *i*th normal mode (in cm^{-1}) and S_i is the Raman scattering activity of the normal mode v_i. f (is a constant equal to 10^{-12}) is a suitably chosen common normalization factor for all peak intensities. *h, k, c,* and *T* are Planck and Boltzmann constants, speed of light and temperature in Kelvin, respectively.

The heteroaromatic structure shows the presence of C–H stretching vibrations above 3000 cm^{-1} which is the characteristic region for ready identification of this structure. In this region, the bands are not affected appreciably by the nature of the substituent [44]. In this study, the last six vibrations are assigned to C–H stretching, which correspond to stretching modes of C–H of ring units. All modes are pure stretching vibrations 100% TED terms. The C–H in-plane bending wavenumbers appear in the range of 1000–1300 cm^{-1} and C–H out-of-plane bending vibration in the range of 750–1000 cm^{-1}. The in-plane C–H bending vibrations were assigned in the range that mentioned above and according to their TED; they are described as mixed modes, generally with C–C vibrations. The out-of-plane C–H vibrations are assigned as pure modes (the TED of all six modes is greater than 86%) and there is a quite good correlation with computed and observed values.

A major coincidence of theoretical values with that of experimental evaluations is found in the symmetric and asymmetric stretching vibrations of the methylene (–CH_2–) moiety. The modes of 62 and 63 are due to the symmetric and asymmetric stretching of CH_2. The computed values

Table 1 The calculated geometric parameters of 4-(thiophene-3-yl-methoxy)phthalonitrile, bond lengths in angstrom, bond angles and selected dihedral angles in degrees

	Exp. [40]	B3LYP
Bond lengths (Å)		
C(1)–C(2)	1.388	1.401
C(1)–C(6)	1.394	1.4
C(1)–O(14)	1.349	1.352
C(2)–C(3)	1.39	1.391
C(3)–C(4)	1.394	1.416
C(3)–C(11)	1.437	1.431
C(4)–C(5)	1.394	1.397
C(4)–C(10)	1.435	1.427
C(5)–C(6)	1.367	1.391
C(10)–N(12)	1.142	1.156
C(11)–N(13)	1.139	1.155
O(14)–C(23)	1.443	1.43
C(15)–C(23)		1.501
C(16)–C(18)		1.365
C(17)–S(20)		1.731
C(18)–S(20)		1.731
C(15)–C(16)		1.432
C(16)–C(17)		1.366
$C–H_{average}$	0.96	1.085
Bond angles (°)		
C(2)–C(1)–C(6)	119.8	119.7
C(2)–C(1)–O(14)	115.3	115.4
C(6)–C(1)–O(14)	124.9	124.9
C(1)–C(2)–C(3)	119.4	120.5
C(1)–C(2)–H(7)	121.7	119.1
C(3)–C(2)–H(7)	118.9	120.4
C(2)–C(3)–C(4)	120.9	120.1
C(2)–C(3)–C(11)	119.1	118.9
C(4)–C(3)–C(11)	120	121
C(3)–C(4)–C(5)	118.6	118.6
C(3)–C(4)–C(10)	122	121.6
C(5)–C(4)–C(10)	119.4	119.8
C(4)–C(5)–C(6)	120.9	121.4
C(4)–C(5)–H(8)	118.6	119
C(6)–C(5)–H(8)	120.5	119.6
C(1)–C(6)–C(5)	120.4	119.8
C(1)–C(6)–H(9)	117.2	121.2
C(5)–C(6)–H(9)	122.3	119
C(1)–O(14)–C(23)	119	119.3
O(14)–C(23)–H(24)	109.2	109.5
O(14)–C(23)–H(25)	107.7	109.5
H(24)–C(23)–H(25)	106.4	108.1
C(4)–C(10)–N(12)	177.6	178.4
C(3)–C(11)–N(13)	179.8	178.7
C(18)–C(16)–H(19)		123.1
C(15)–C(17)–S(20)		111.7
C(15)–C(17)–H(21)		127.9
S(20)–C(17)–H(21)		120.4
C(16)–C(18)–S(20)		111.6
C(16)–C(18)–H(22)		128.2
S(20)–C(18)–H(22)		120.2
C(17)–S(20)–C(18)		91.5
O(14)–C(23)–C(15)		109.1
C(16)–C(15)–C(17)		112.4
C(16)–C(15)–C(23)		122.3
C(15)–C(23)–H(24)		110.4
C(15)–C(23)–H(25)		110.4
C(17)–C(15)–C(23)		125.3
C(15)–C(16)–C(18)		112.8
C(15)–C(16)–H(19)		124.1
Dihedral angles (°)		
C(4)–C(10)–N(12)–C(5)		178.4
C(3)–C(11)–N(13)–C(2)		178.7
C(1)–O(14)–C(23)–H(24)		−59.1
C(1)–O(14)–C(23)–H(25)		59.2
C(16)–C(15)–C(23)–H(24)		59.7
C(16)–C(15)–C(23)–H(25)		−59.7
C(17)–C(15)–C(23)–H(24)		−120.3
C(17)–C(15)–C(23)–H(25)		120.3
C(15)–C(23)–O(14)–C(1)		180.0
S(20)–C(17)–C(15)–C(23)		180.0
C(2)–C(1)–O(14)–C(23)		180.0

for symmetric and asymmetric stretching vibrations show good agreement with obtained data (2875 cm^{-1} in FT-IR and 2883 cm^{-1} in FT-Raman for symmetric stretching and 2941 cm^{-1} in FT-IR and FT-Raman for symmetric stretching). The TED contribution of the both stretching modes indicates that these are highly pure modes. An attempt of the assignment of this non-fundamental band leads us to propose it as combination vibration. The deformation vibrations of $–CH_2–$ group (scissoring, wagging, twisting, and rocking) contribute to several normal modes in the low frequency region. The vibration obtained at ca. 990 cm^{-1} (mode no 39) is assigned to CH_2 rocking and calculated at 1018 cm^{-1} as a pure mode. Likewise, the pure vibration mode of 47 is due to the twisting of CH_2. The CH_2 scissoring was obtained at 1489 cm^{-1} (FT-IR) and calculated at 1478 cm^{-1}, after scaling procedure. The vibration modes of 51 and 52 were assigned to CH_2 wagging. On the contrary other CH_2 vibrations, both of these modes are contaminated with other vibrations, as can be seen in Table 2.

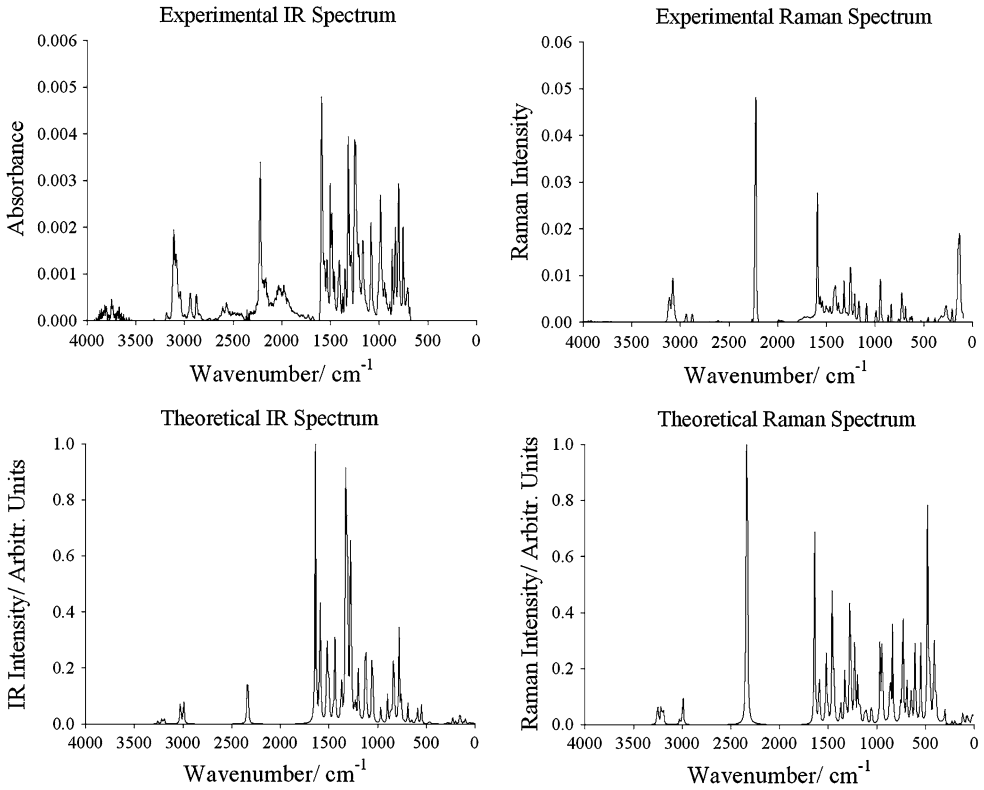

Fig. 2 The observed and simulated Infrared and Raman spectra of present compound

The ring stretching vibrations are very much important in the spectrum of benzene derivatives and are highly characteristic of the aromatic ring itself. Bands between 1400 and 1650 cm^{-1} in benzene derivatives are assigned to these modes. In general, the bands are of variable intensity and observed at 1625–1590, 1590–1575, 1540–1470, 1460–1430, and 1380–1280 cm^{-1} from the frequency ranges given by Varsanyi [45] for the five bands in the region. Hence, in this work, the wavenumbers observed in the FT-IR spectrum at 1559 and 1594 cm^{-1} and in FT-Raman spectrum at 1547 and 1568 cm^{-1} are assigned to C–C stretching vibrational modes. The vibration modes of 56 and 59 which were recorded at 1510 (1504 cm^{-1} in FT-IR) and 1596 cm^{-1} as a weak and sharp band in FT-Raman spectrum, are due to the C–C stretching and in-plane C–H bending of ring 2 (R2), respectively. The observed band at 1462 cm^{-1} is due to C–C stretching of ring 1 (R1). The TED contribution of this mode (79%) indicates that this is ca. pure mode. The same vibration appears in the FT-Raman spectrum at 1464 cm^{-1}. C–C in-plane and out-of-plane bending modes are the modes associated with smaller force constants than the stretching ones, and hence assigned to lower frequencies. The theoretically calculated CCC in-plane bending and out-of-plane bending modes have been found to be consistent with the recorded spectral values. The TED of these vibrations is mixed modes as it is evident from Table 2, except mode 28 which demonstrates the out-of-plane CCC vibration of R2.

Identification of C–S stretching vibration is difficult and also uncertain. The recorded four peaks by Klots et al. [8] which are 608.8, 753.5, 839.5, and 872.8 cm^{-1} are assigned to C–S stretching by Singh et al. [9] according to potential energy distribution (PED) obtained from DFT calculations. In this study, we have assigned five bands due to the C–S stretching based on the TED calculations, and obtained two bands (mode 29 and 32) which show excellent agreement with computed values. As can be seen from Table 2, for C–S stretching modes the calculated unscaled wavenumbers show better agreement than scaled ones. However, the scaled wavenumbers are coincident with experimental results of liquid thiophene and thiophene in acetonitrile [46]. All C–S stretching vibrations are assigned as mixed modes which are contaminated with in-plane ring bending vibrations. The calculated band at 448 cm^{-1} (unscaled value is 455 cm^{-1}) was assigned to out-of-plane C–S–C bending with TED contribution of 88%. This band was obtained at 452.3, 450.1 cm^{-1} by Klots et al. [8] and Pasternya et al. [46], respectively.

The sharp band in the region of 2210–2270 cm^{-1} is easily assigned to the characteristic C≡N stretching mode [47]. Zeng et al. [48] assigned the cyano stretching vibration at 2233 cm^{-1} for 3,5-bis(3,4-dicyanophenoxy)aniline and in the range of 2229–2249 cm^{-1} for hydroxy-containing phthalonitrile model compounds [49]. In this study, the very strong band at 2231 cm^{-1} in FT-Raman spectrum (2222 cm^{-1} in FT-IR) and calculated band at 2244 cm^{-1}

Table 2 Comparison of the calculated and experimental vibrational spectra and proposal assignments of title compound

	Experimental		6-311++G(d, p)/B3LYP				TED (≥10%)
	FT-IR	FT-Raman	U. Waven.	S. Waven.	I_{IR}	S_{Ra}	Assignments
1			11	10	0.102	1.015	γCH_2-R1 (95)
2			25	24	1.268	1.022	Butterfly
3			56	55	1.667	0.747	βR1-R2
4			78	77	0.001	3.751	γCH_2 (82)
5			98	97	3.224	0.350	γCCC_{R2} (42) + γCCN (31)
6			117	115	1.575	6.097	wCCN (96)
7		141 s	149	146	3.217	0.316	β{CCO + COC} (41) + βCN (21) + $\beta CCC_{10,11}$ (18)
8			158	155	6.588	0.102	R2 umbrella (86)
9			199	196	1.776	2.583	βCOC (25) + βCN (24) + $\beta CCC_{10,11}$ (13)
10		215 vw	227	223	4.276	3.036	γCH_2 (74)
11			268	263	0.688	0.067	γCOC (35) + γCCN (19) + γCCC_{R2} (15)
12		273 vw	283	278	1.550	2.163	βC–CH_2 (28) + βCCO (16) + νO–CH_2 (10)
13		384 vw	395	388	0.292	1.099	γCCC_{R2} (54) + γCCN (34)
14			414	407	0.280	3.396	βCCC_{R2} (31) + $\nu CC_{10,11}$ (20) + βCCN (10)
15			455	448	0.051	1.159	γCSC (88)
16			462	454	1.011	1.124	γCCC_{R2} (40) + γCCN (35)
17		458 vw	467	459	1.033	0.982	β{CCO + COC} (61)
18			480	472	0.753	8.755	βCCN (40) + βCCC_{R2} (16)
19			549	540	0.690	1.381	βCCN (41) + $R1_{breath.}$ (11)
20			551	542	13.018	3.277	γCCN (75)
21			592	582	10.999	0.181	γCCC_{R1} (56) + rCH_2 (17) + γCH_{R1} (10)
22			608	597	2.626	6.731	ν_{sym}CS (18) + βSCC (14) + βCSC (18)
23		628 vw	643	632	1.052	1.677	γCCN (34) + γCCC_{R2} (26) + γCH_{R2} (22)
24		644 vw	653	642	2.375	2.283	βCCN (63)
25			692	680	14.240	0.027	γCH_{R1} (99)
26		689 vw	693	681	0.726	4.858	νCS (21) + βCCC_{R1} (18)
27	707 w		733	721	1.414	16.317	νCC_{R2} (30) + νCC_{10} (19) + βCCC_{R2} (19)
28		730 m	744	731	0.063	0.776	γCCC_{R2} (79)
29	755 m		758	745	19.357	2.574	β{CCO + COC + OCC} (22) + βCCC_{R2} (19) + ν_{asym}CS (13)
30		760 vw	784	770	65.009	0.134	γCH_{R1} (90)
31	802 m		832	818	38.723	0.110	γCH_{R2} (86)
32	834 m	838 m	840	826	27.602	14.437	νCS (49) + βSCC (34)
33			865	850	11.849	10.385	νCS (56) + βSCC (36)
34	868 m	867 vw	885	870	0.091	0.497	γCH_{R1} (92)
35			901	885	19.174	0.181	γCH_{R2} (89)
36			946	930	1.169	21.712	νCC_{R2} (27) + νO–CH_2 (12) + νCC_{11} (10) + νCO (10)
37	947 w	953 vw	966	950	2.276	0.211	γCH_{R2} (87)
38			969	952	10.268	16.593	νCC_{R1} (30) + νC–CH_2 (15) + {βCCC (16) + βCH (14)}$_{R1}$
39	989 s	990 vw	1035	1018	0.145	0.157	rCH_2 (86)
40			1054	1037	72.035	7.403	νO–CH_2 (54) + νCC_{R2} (19)
41	1086 m	1093 m	1107	1088	6.791	5.047	βCH_{R2} (81) + νCC_{R1} (15)
42			1123	1104	91.302	5.455	{βCH (27) + βCCC (15)}$_{R2}$ + νCC_{11} (13)
43			1176	1156	1.560	9.840	βCH_{R1} (50) + νC–CH_2 (21)
44	1170 m	1167 w	1197	1177	41.239	17.079	βCH_{R2} (52) + νCC_{11} (13) + νCC_{R2} (12)
45	1209 m	1213 m	1226	1205	12.480	37.976	{βCH (33) + νCC (20)}$_{R2}$ + νCC_{10} (23)
46			1237	1216	7.902	2.692	{βCH (67) + νCC (10)}$_{R1}$
47			1261	1240	1.185	7.259	tCH_2 (89)

Table 2 continued

	Experimental		6-311++G(d, p)/B3LYP				TED (≥10%)
	FT-IR	FT-Raman	U. Waven.	S. Waven.	I_{IR}	S_{Ra}	Assignments
48	1254 vs	1258 m	1276	1254	173.638	73.705	$\{\beta CH\ (41) + \nu CC\ (24)\}_{R2} + \nu CO\ (11)$
49			1314	1292	222.126	8.690	$\{\nu CC\ (42) + \beta CH\ (33)\}_{R2} + \nu CO\ (15)$
50	1319 vs	1324 m	1329	1306	133.278	22.368	$\nu CC_{R2}\ (58) + \nu CO\ (19)$
51	1375 w	1382 w	1373	1349	41.523	15.008	$wCH_2\ (28) + \{\beta CH\ (28) + \nu CC\ (16)\}_{R1}$
52	1411 w	1414 m	1436	1412	62.581	24.452	$wCH_2\ (20) + \nu CC_{R1}\ (17) + \{[\nu CC + \beta CH]\ (10)\}_{R2}$
53			1454	1429	6.986	13.652	$\{\nu CC\ (32) + \beta CH\ (12)\}_{R2}$
54	1462 w	1464 w	1458	1434	5.402	78.025	$\nu CC_{R1}\ (79)$
55	1489 m		1503	1478	50.932	13.370	$\rho CH_2\ (84)$
56	1504 s	1510 w	1522	1496	63.840	55.122	$\{\nu CC\ (33) + \beta CH\ (30)\}_{R2}$
57	1559 w	1547 w	1588	1561	73.480	22.963	$\nu CC_{R2}\ (47) + \nu CC_{R1}\ (15)$
58	1594 vs	1568 w	1596	1568	27.599	24.465	$\nu CC_{R1}\ (42) + \nu CC_{R2}\ (15)$
59		1596 s	1640	1612	186.830	155.371	$\{\nu CC\ (65) + \beta CH\ (15)\}_{R2}$
60	2222 m	2231 vs	2334	2236	43.000	793.248	$\nu C{\equiv}N\ (88) + \nu CC_{10}\ (11)$
61			2342	2244	9.294	373.495	$\nu C{\equiv}N\ (88) + \nu CC_{11}\ (11)$
62	2875 w	2883 vw	2992	2866	20.400	203.880	$\nu_{sym}CH_2\ (99)$
63	2941 w	2941 vw	3025	2898	18.622	43.473	$\nu_{asym}CH_2\ (100)$
64	3042 w		3192	3058	3.331	88.508	$\nu CH_{R1}\ (100)$
65			3198	3064	1.676	57.681	$\nu CH_{R2}\ (100)$
66			3212	3077	0.887	69.774	$\nu CH_{R2}\ (100)$
67	3081 w	3080 m	3219	3084	3.220	106.349	$\nu CH_{R2}\ (100)$
68	3111 m	3114 w	3247	3111	0.536	158.520	$\nu CH_{R1}\ (100)$
69			3262	3125	1.989	72.844	$\nu CH_{R1}\ (100)$

U. Waven., S. Waven. unscaled wavenumbers, scaled wavenumbers; *R1, R2* ring 1, 2; ν-ν_{sym}–ν_{asym} stretching-symmetric stretching–asymmetric stretching; β in-plane bending; γ out-of-plane bending; ρ scissoring; t twisting; r rocking; w wagging

are assigned to C≡N stretching vibrations which have good correlation with literature data given above. Because of the wide spectral range and poor IR and Raman intensities C–C–C≡N bending does not offer practical application as a characteristic frequency [47]. The in-plane and out-of-plane ring-C≡N vibrations and remaining modes such as C–O, O–CH_2 are gathered in Table 2.

NMR calculations

The experimental ^1H and ^{13}C NMR spectra of 4-(thiophene-3-ylmethoxy)phthalonitrile are shown in Fig. 3. The recorded and calculated ^1H and ^{13}C chemical shifts in the $CDCl_3$ solution are gathered in Table 3. The atom positions were numbered as in Fig. 1. The isotropic chemical shifts are frequently used as an aid in identification of reactive ionic species. It is recognized that accurate predictions of molecular geometries are essential for reliable calculations of magnetic properties. Therefore, full geometry optimization of present compound was performed at the gradient corrected density functional level of theory using the hybrid B3LYP method. Then, GIAO ^1H and ^{13}C chemical shift calculations of the compound has been made by same method and 6-311++G(d,p) basis set. The isotropic shielding values were used to calculate the isotropic chemical shifts δ with respect to tetramethylsilane (TMS), $\left(\delta^X_{iso} = \sigma^{TMS}_{iso} - \sigma^X_{iso}\right)$. Comparison between experimental and theoretical NMR chemical shifts provides practical information on the chemical structure and conformation of compounds. This usefulness is largely due to empirical structure chemical shift correlations.

It is clear from Table 3 that the agreement with experimental data is good, even the trends in relative values are well reproduced. The largest differentiation in ^{13}C chemical shifts is observed for C(5), amounting to about 16 ppm. The differentiation found in ^1H, on the other hand, is only of a few tenths of ppm. Signals for protons were observed at 5.207–7.747 ppm. Two 5,207 signals result from methylene group (H(24) and H(25)). The H atom is the smallest of all atoms and mostly localized on the periphery of molecules; therefore their chemical shifts would be more susceptible to intermolecular interactions in the aqueous solutions as compared to that for other heavier atoms.

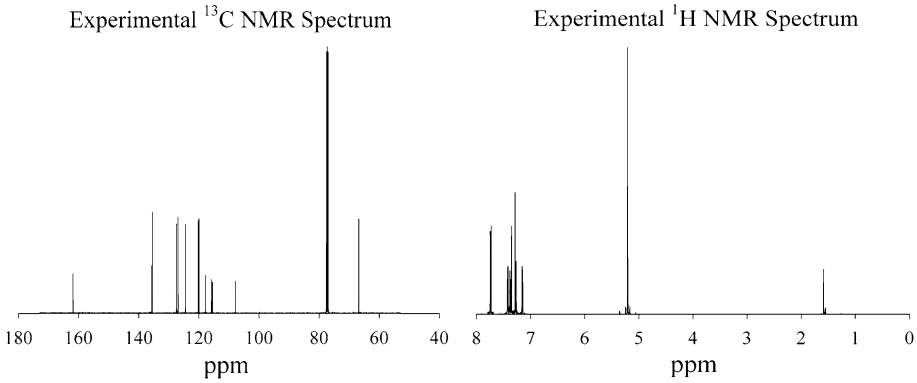

Fig. 3 The experimental ^{13}C and ^{1}H NMR spectra of 4-(thiophene-3-ylmethoxy)phthalonitrile (in $CDCl_3$ solution)

Table 3 Experimental and theoretical, ^{1}H and ^{13}C NMR isotropic chemical shifts (with respect to TMS) of title compound by DFT (B3LYP) method

Atom	Experimental	B3LYP
C(1)	161.83	167.96
C(2)	120.14	130.07
C(3)	117.74	121.26
C(4)	107.86	111.20
C(5)	127.42	143.83
C(6)	120.14	118.43
C(10)	115.85	123.15
C(11)	115.46	122.15
C(15)	135.49	141.41
C(16)	126.92	127.82
C(17)	119.91	129.65
C(18)	124.42	137.76
C(23)	66.81	70.63
H(7)	7.729	7.834
H(8)	7.747	8.073
H(9)	7.158	7.340
H(19)	7.148	7.280
H(21)	7.349	7.757
H(22)	7.287	7.629
H(24)	5.207	5.362
H(25)	5.207	5.362

The relations between the experimental ^{1}H and ^{13}C chemical shifts (δ_{exp}) and magnetic isotropic shielding tensors (σ) are usually linear and described by the following equation:

$$\delta = a + b\sigma$$

In this study, the following linear relationships were obtained for ^{1}H and ^{13}C chemical shifts.

$$^{1}\mathrm{H} : \delta_{cal}(\mathrm{ppm}) = 1.0417\delta_{exp} - 0.0599 (R^2 = 0.9905)$$

$$^{13}\mathrm{C} : \delta_{cal}(\mathrm{ppm}) = 1.0435\delta_{exp} + 1.3480 (R^2 = 0.9517)$$

The performances of the B3LYP method with respect to the prediction of the relative shielding within the molecule were quite close. However, ^{1}H calculations gave a slightly better coefficient and lower standard error ($R^2 = 0.9905$) than for ^{13}C chemical shifts. The correlations between the experimental and calculated chemical shifts obtained by DFT method are shown in Fig. 4.

Based on the ^{1}H and ^{13}C chemical shifts data collected in Table 3 one can deduce that qualitatively the ^{13}C and ^{1}H NMR chemical shifts of 4-(thiophene-3-ylmethoxy)phthalonitrile are described fairly well by the selected DFT method combined with the basis set. As can be seen from Table 3 and Fig. 4, there is a good agreement between experimental and theoretical chemical shift results for the title compound.

UV spectrum and electronic properties

The UV spectrum of 4-(thiophene-3-ylmethoxy)phthalonitrile, shown in Fig. 5, was measured in tetrahydrofuran (THF) solution. It is observed that the absorption bands are centered at 259, 296, and 306 nm for THF. The experimental and computed electronic values, such as absorption wavelength, excitation energies, frontier orbital energies, and oscillator strengths are tabulated in Table 4. The agreement between theoretical and experimental data is

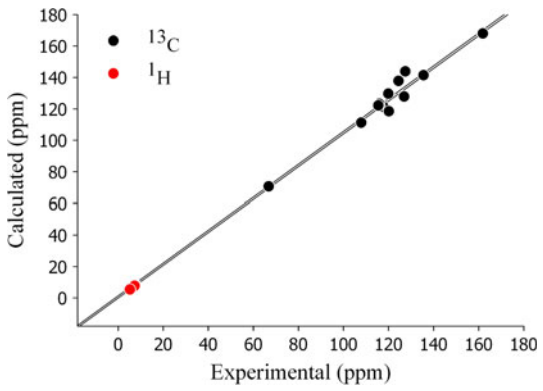

Fig. 4 Plot of the computed versus experimental ^{1}H and ^{13}C relative chemical shifts of 4-(thiophene-3-ylmethoxy)phthalonitrile (in $CDCl_3$ solution)

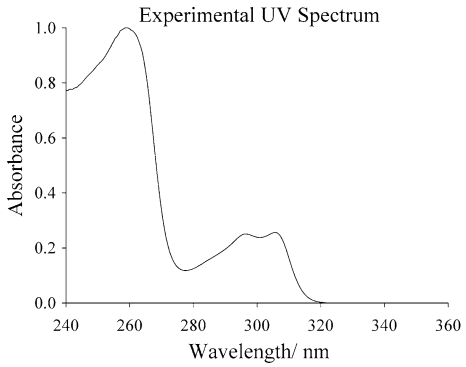

Fig. 5 The experimental UV spectrum of studied compound (in THF)

quite acceptable. In order to understand electronic transitions of compound, TD–DFT calculations on electronic absorption spectra in THF were performed. Both the highest occupied molecular orbital (HOMO) and the lowest unoccupied molecular orbital (LUMO) are the main orbital taking part in chemical reaction. The HOMO energy characterizes the ability of electron giving, LUMO characterizes the ability of electron accepting, and the gap between HOMO and LUMO characterizes the molecular chemical stability [50]. The features of the HOMO and LUMO can be seen in Fig. 6. The energy gap between the highest occupied and the lowest unoccupied molecular orbitals, is a critical parameter in determining molecular electrical transport properties because it is a measure of electron conductivity. According to Fig. 6, the HOMO of steady compound presents a charge density localized on the sulfur atom where the LUMO is characterized by a charge distribution on some carbon atoms of the ring 2. The experimental band at 259 nm is attributed mainly to a HOMO → LUMO transition where the experimental band found at 295 nm can be assigned mainly to a transition

Table 4 Experimental and calculated wavelengths λ (nm), excitation energies (eV), oscillator strengths (f), absolute energies (Hartree), frontier orbital energies (a.u.), and dipole moment (Debye) in tetrahydrofuran (THF) solution

Exp. (in THF) λ (nm)	B3LYP/DFT (in THF) λ (nm)	E (eV)	f	E_{total}		
259	282 (HOMO → LUMO)	4.4014	0.0762	$E_{\text{HOMO}} = -0.24764$	$E_{\text{LUMO}} = -0.08700$	$\Delta E = -0.16064$
295	294 (HOMO −1 → LUMO +1)	4.2184	0.0962	$E_{\text{HOMO +1}} = -0.25792$	$E_{\text{LUMO −1}} = -0.06181$	$\Delta E = -0.19611$
306	316	3.9254	0.0003	μ (D) = 11.6083		

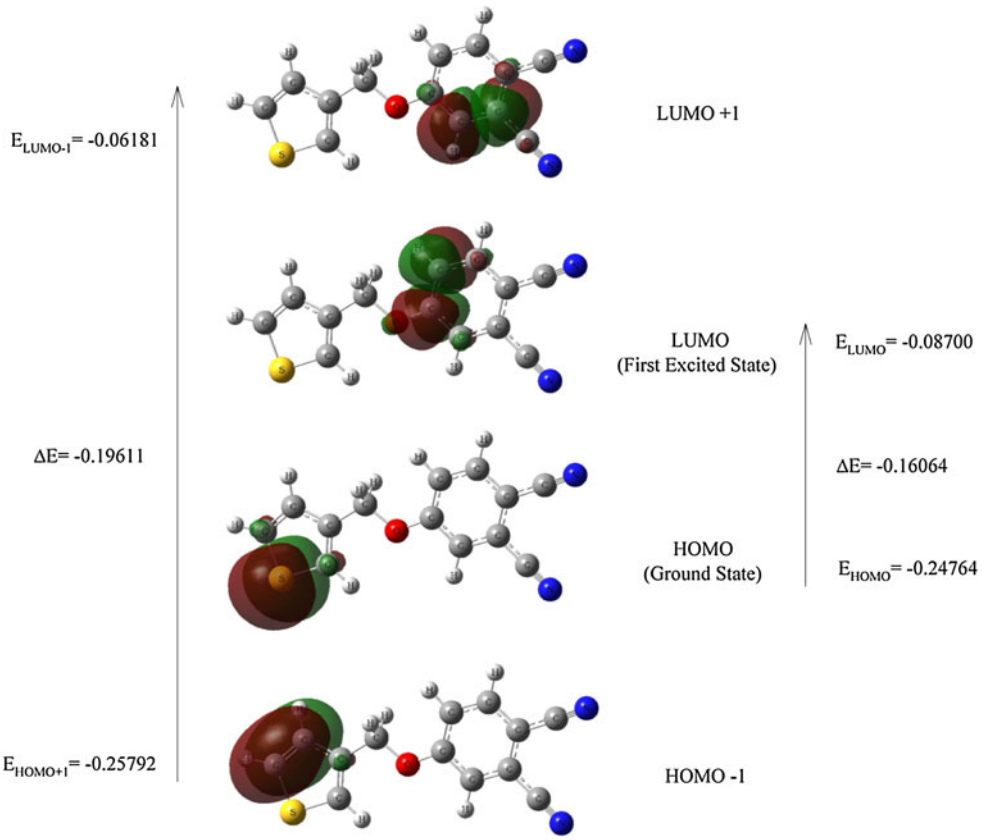

Fig. 6 The frontier and second frontier molecular orbitals of studied compound

from HOMO −1 → LUMO +1. It should be noted that other one-electron excitations may also contribute to describe this observed band. It can be seen from Fig. 6 that HOMO present a nonbonding character for some atoms, including sulfur and carbon atoms of R1. The HOMO −1 could be characterized as a π-bonding molecular orbital between a pair of ring atoms. Finally, the LUMO and LUMO +1 exhibit a π-antibonding character between some pair of R2, with some minor contribution from other carbon atoms.

Conclusion

The 4-(thiophene-3-ylmethoxy)phthalonitrile was synthesized and several properties were studied using experimental techniques and tools derived from the density functional theory. A conformational analysis was carried out by means of molecular dynamics simulations. The optimized geometric parameters of molecule were interpreted and compared with the earlier reported experimental values for a similar compound. According to the computed results the phthalonitrile group is coplanar with the four-atom bridge (C1–O14–C23–C15) to the thiophene group. The vibrational FT-IR and FT-Raman spectra of molecule were recorded and assigned with the aid of the experimental and computed vibrational wavenumbers and their TED. The magnetic properties of the title compound were observed and calculated. The chemical shifts were compared with experimental data, showing a very good agreement both for ^{13}C and ^{1}H. However, ^{1}H calculations gave a slightly better coefficient and lower standard error than for ^{13}C chemical shifts. The electronic properties were also calculated and experimental electronic spectrum was recorded with help of UV–Vis spectrometer. The maxima absorption wavelengths were observed at 259, 295, and 306 nm. The two characteristic bands at 259 and 295 nm are possibly due to a $\pi \rightarrow \pi^*$ transition. The band at 306 nm is predicted as an $n \rightarrow \pi^*$ transition. The comparison of the predicted bands with the experimental bands was done and shows an acceptable general agreement.

In summary, a very complete characterization of studied novel compound was given in this paper. It has been shown; moreover, hybrid density functional calculations are able to supply a variety of very reliable molecular properties.

References

1. Steinkopf W (1941) Die Chemie des Tiophens CA 39(16–482):61
2. Reddinger JL, Reynolds JR (1999) Adv Polym Sci 145:57122
3. McQuade DT, Pullen AE, Swager TM (2000) Chem Rev 100:2537
4. Kerman I, Toppare L, Yilmaz F, Yagci Y (2005) J Polym Sci A A42:509
5. Yilmaz F, Sel O, Cirpan A, Toppare L, Hepuzer Y, Yagci Y (2004) J Polym Sci A A41:401
6. Kwiatkowski JS, Leszczynski J, Teca I (1997) J Mol Struct 436–437:451
7. Ramirez FJ, Hernandez V, Lopez Navarrete JT (1994) J Comput Chem 15:405
8. Klots TD, Chirico RD, Steele WV (1994) Spectrochim Acta A50:765
9. Singh DK, Srivastava SK, Ojha AK, Asthana BP (2008) J Mol Struct 892:384
10. Rico M, Orza JM, Morcillo J (1965) Spectrochim Acta 21:689
11. McKeown NB (1998) Phthalocyanine materials: synthesis, structure and function. Cambridge University Press, Cambridge
12. Leznoff CC, Lever ABP (1996) Phthalocyanines: properties and applications, vol 1–4. VCH, New York
13. Mack J, Kobayashi N, Stillman MJ (2006) J Porphyr Phthalocyanines 10:1219
14. Sakamoto K, Kato T, Okumura EO, Watanabe M, Cook MJ (2005) Dyes Pigm 64(1):63
15. Arvand M, Pourhabib A, Shemshadi R (2007) Anal Bioanal Chem 387(3):1033
16. Chen JC, Chen NS, Huang JF (2006) Inorganic Chem Commun 9(3):313
17. Knawby DK, Swager TM (1997) Chem Mater 9:535–538
18. Moser FH, Thomas AL (1983) The phthalocyanines, vol 1 & 2. CRC Press, Boca Raton, Florida
19. Keller TM, Price TK (1982) J Macromol Sci Chem 18:931
20. Keller TM (1992) Polymer Prepr 33:422
21. Burchill PJ (1994) J Polym Sci A 32:1
22. Keller TM, Griffith JR (1980) ACS Org Coat Plast Chem Prepr 43:804
23. Woehrle D, Schulte B (1988) Makromol Chem 189:1167
24. Woehrle D, Schulte B (1989) Makromol Chem 190:1573
25. Frisch MJ, Trucks GW, Schlegel HB, Scuseria GE, Robb MA, Cheeseman JR, Zakrzewski VG, Montgomery JA Jr, Stratmann RE, Burant JC, Dapprich S, Millam JM, Daniels AD, Kudin KN, Strain MC, Farkas O, Tomasi J, Barone V, Cossi M, Cammi R, Mennucci B, Pomelli C, Adamo C, Clifford S, Ochterski J, Petersson GA, Ayala PY, Cui Q, Morokuma K, Malick DK, Rabuck AD, Raghavachari K, Foresman JB, Cioslowski J, Ortiz JV, Baboul AG, Stefanov BB, Liu G, Liashenko A, Piskorz P, Komaromi I, Gomperts R, Martin RL, Fox DJ, Keith T, Al-Laham MA, Peng CY, Nanayakkara A, Challacombe M, Gill PMW, Johnson B, Chen W, Wong MW, Andres JL, Gonzalez C, Head-Gordon M, Replogle ES, Pople JA (2002) GAUSSIAN 03, Revision A.9. Gaussian, Inc., Pittsburgh
26. Obirai J, Nyokong T (2005) Electrochim Acta 50:5427
27. Becke AD (1993) J Chem Phys 98:5648
28. Lee C, Yang W, Parr RG (1988) Phys Rev B37:785
29. Karabacak M, Cinar M, Coruh A, Kurt M (2009) J Mol Struct 919:26
30. Karabacak M, Kurt M, Cinar M, Coruh A (2009) Mol Phys 107(3):253
31. Karabacak M, Cinar M, Ermec S, Kurt M (2010) J Raman Spectrosc 41(1):98
32. Baker J, Jarzecki AA, Pulay P (1998) J Phys Chem A102:1412
33. Rauhut G, Pulay P (1995) J Phys Chem 99:3093
34. Ditchfield R (1972) J Chem Phys 56:5688
35. Wolinski K, Hinton JF, Pulay P (1990) J Am Chem Soc 112:8251
36. Runge E, Gross EKU (1984) Phys Rev Lett 52:997
37. Petersilka M, Gossmann UJ, Gross EKU (1966) Phys Rev Lett 76:1212
38. Bauernschmitt R, Ahlrichs R (1996) Chem Phys Lett 256:454

39. Jamorski C, Casida ME, Salahub DR (1996) J Chem Phys 104:5134
40. Dincer M, Agar A, Akdemir N, Agar E, Ozdemir N (2004) Acta Cryst E60:o79
41. Sundaraganesan N, Ilakiamani S, Saleem H, Wojciechowski PM, Michalska D (2005) Spectrochim Acta A 61:2995
42. Keresztury G, Holly S, Varga J, Besenyei G, Wang AY, Durig JR (1993) Spectrochim Acta 49A:2007
43. Keresztury G, Chalmers JM, Griffith PR (eds) (2002) Raman spectroscopy: theory, hand book of vibrational spectroscopy, vol 1. Wiley, New York
44. Silverstein M, Basseler GC, Morill C (1981) Spectrometric identification of organic compounds. Wiley, New York
45. Varsanyi G (1974) Assignments of vibrational spectra of 700 benzene derivatives. Wiley, New York
46. Pasternya K, Wrzalik R, Kupka T, Pasterna G (2002) J Mol Struct 614:297–304
47. Lin–Vien D, Colthup NB, Fateley WG, Grasselli JG (1991) The handbook of infrared and Raman characteristic frequencies of organic molecules. Academic Press, Boston, MA
48. Zeng K, Zhou K, Tang WR, Tang Y, Zhou HF, Liu T, Wang YP, Zhou HB, Yang G (2007) Chin Chem Lett 18:523–526
49. Zeng K, Zhou K, Zhou S, Hong H, Zhou H, Miao YWP, Yang G (2009) Eur Polym J 45:1328–1335
50. Fukui K (1982) Science 218:747